THE JOURNAL OF BIOLOGICAL CHEMISTRY VOL. 289, NO. 12, pp. 8473–8483, March 21, 2014

Pleiotropic Effects of Cavin-1 Deficiency on Lipid Metabolism*

Received for publication, December 27, 2013, and in revised form, February 6, 2014 Published, JBC Papers in Press, February 7, 2014, DOI 10.1074/jbc.M113.546242

Shi-Ying Ding[‡], Mi-Jeong Lee[§¶], Ross Summer[§‖], Libin Liu[‡], Susan K. Fried[§¶1], and Paul F. Pilch[‡§2]

From the [‡]Departments of Biochemistry and [§]Medicine, [¶]Division of Endocrinology, Diabetes and Nutrition, and [‖]Pulmonary Center, Department of Medicine, Boston University School of Medicine, Boston, Massachusetts 02118

Background: Cavin-1 expression is critical for the formation of caveolae, exceptionally abundant structure in adipocytes.
Results: Adipocytes from *cavin-1*-null mice are markedly dysfunctional exhibiting decreased insulin-dependent glucose uptake, fatty acid uptake, and lipolysis.
Conclusion: Cavin-1/caveolae have major roles in the regulation of adipocyte metabolism.
Significance: Fat cell cavin-1/caveolae functions are important for organismal lipid metabolism in mice and men.

Mice and humans lacking caveolae due to gene knock-out or inactivating mutations of *cavin-1/PTRF* have numerous pathologies including markedly aberrant fuel metabolism, lipodystrophy, and muscular dystrophy. We characterized the physiologic/metabolic profile of *cavin-1* knock-out mice and determined that they were lean because of reduced white adipose depots. The knock-out mice were resistant to diet-induced obesity and had abnormal lipid metabolism in the major metabolic organs of white and brown fat and liver. Epididymal white fat cells from *cavin-1*-null mice were small and insensitive to insulin and β-adrenergic agonists resulting in reduced adipocyte lipid storage and impaired lipid tolerance. At the molecular level, the lipolytic defects in white fat were caused by impaired perilipin phosphorylation, and the reduced triglyceride accumulation was caused by decreased fatty acid uptake and incorporation as well as the virtual absence of insulin-stimulated glucose transport. The livers of *cavin-1*-null mice were mildly steatotic and did not accumulate more lipid after high-fat feeding. The brown adipose tissues of *cavin-1*-null mice exhibited decreased mitochondria protein expression, which was restored upon high fat feeding. Taken together, these data suggest that dysfunction in fat, muscle, and liver metabolism in *cavin-1*-null mice causes a pleiotropic phenotype, one apparently identical to that of humans lacking caveolae in all tissues.

Early electron micrographs of adipocytes showed the abundant presence of small membrane structures, then called pinosomes or pinocytic vesicles, at or near the fat cell surface (1–3). We now know these morphological features to be caveolae, and fat cells abundantly express caveolin-1 (Cav1)[3] (4, 5), a major structural protein of caveolae (6), whose discovery helped initiate the molecular era of caveolae biology in adipocytes (reviewed in Refs. 7, 8) and other cells (9–11). More recent morphological studies have shown that ~50% of the adipocyte cell surface area consists of caveolae (12, 13). In addition to Cav1, caveolae from fat cells, and non-muscle cells that have caveolae, express caveolin-2 (Cav2), like Cav1, a small (<178 amino acids) integral membrane protein and three members of the cavin family of peripheral, caveolae-associated membrane proteins (9, 11), namely cavin-1 (14–16), cavin-2 (10, 13, 17), and cavin-3 (17, 18). Although it has not been experimentally determined in every tissue, Cav1 (Cav3 in muscle) and cavin-1 are required for caveolae formation (9, 11), cavin-2 affects caveolae shape and abundance in a tissue-sensitive manner (20), whereas the expression of Cav2 (19) and cavin-3 appears to not be required for caveolae structures (20).[4] In addition, cholesterol is a requisite lipid component of these domains (21).

The abundance of caveolae in adipocytes suggests that they may play a particular role in their most active functions, namely to take up and store fatty acids (FA) as triglycerides (TG) in the fed state and hydrolyze TG and release FA in response to fasting/starvation and exercise (8). The trafficking of high concentrations of FA in and out of fat cells poses a potential toxicity problem because FA are mild detergents capable of disrupting the adipocyte plasma membrane (22), but caveolae are detergent-resistant membrane domains (23) that can function to buffer the effects of FA. In fact, data from cells expressing caveolins/caveolae support the FA buffering function of caveolins/caveolae that protects against FA cytotoxicity as compared with cells that do not have caveolins, and in addition, caveolins modulate the rate of transmembrane FA flux (24–26). Data from mice lacking caveolins/caveolae due to gene knock-out experiments (15, 27, 28) as well as essentially identical data from functionally inactivating mutations in human caveolar proteins (29–33) document multiple effects of caveolae deficiency on overall fuel metabolism as well as on the regulation of adipocyte lipid levels, thus begging the question of the cellular and molecular basis for these pathologies.

To address aspects of the mechanism(s) underlying the dysregulation of metabolism due to caveolae deficiency, we carried out a series of *in vivo* and *in vitro* experiments examining the

* This work was supported, in whole or in part, by Grants R01 DK097708 and R01 DK092942 (to P. F. P.); R01 DK080448 and P30 DK046200 (to S. K. F.); and R01 HL105490 (to R. S.) from the National Institutes of Health.
[1] To whom correspondence may be addressed: Division of Endocrinology, Diabetes, and Nutrition, Department of Medicine, Boston University School of Medicine. 650 Albany St., EBRC-810, Boston, MA 02118. Tel.: 617-638-7110; E-mail: skfried@bu.edu.
[2] To whom correspondence may be addressed: Department of Biochemistry, Boston University School of Medicine. 72 E. Concord St., Boston, MA 02118. Tel.: 617-638-4044; Fax: 617-638-4208; E-mail: ppilch@bu.edu.
[3] The abbreviations used are: Cav1, caveolin-1; PTRF, RNA polymerase I transcription release factor; KO, knock-out; CD, chow diet; HFD, high fat diet; FA, fatty acids; TG, triglycerides; BAT, brown adipose tissue.

[4] L. Liu, B. J. Honeyman, and P. F. Pilch, unpublished data.

metabolic properties of several tissues from *cavin-1*-null mice. We find that the white adipose tissue of the knock-out mice contains small fat cells, is fibrotic and macrophage infiltrated. Isolated white adipocytes from the knock-out respond poorly to β-adrenergic and insulin stimuli and show marked inability to take up and store fatty acids. Brown adipose tissue (BAT) mass is relatively normal in the knock-out, but brown adipocytes are smaller and express low levels of uncoupling protein 1 (UCP1). Livers from the knock-out mice are mildly steatotic. Remarkably, the knock-out mice are resistant to diet-induced obesity and show no exacerbation of the above noted metabolic abnormalities upon high fat feeding. Thus, cavin-1 deficiency results in altered metabolic flux among multiple tissues, which suggests a role of cavin-1 in the coordination of peripheral glucose and fatty acid storage and utilization.

EXPERIMENTAL PROCEDURES

Experimental Animals—Cavin-1$^{-/-}$ mice were created as described on a C57BL/6N × sv129 genetic background (15) and were backcrossed for at least 8 generations with the C57 black lineage. The mice used in the present study were homozygous male *cavin-1*$^{-/-}$ and their wild-type (WT) littermates generated from breeding of *cavin-1*$^{+/-}$ mice. Animals were maintained in a pathogen-free animal facility at 21 °C under a 12-h light/12-h dark cycle with access to a chow diet (CD, 2918; Harlan Teklad Global Diet, Madison, WI). For dietary alterations, mice were individually housed and fed with a high-fat diet (HFD, 45% kcal in fat, D12492; Research Diets, New Brunswick, NJ), or chow, starting at the age of 8 weeks and continued for 12 weeks. Body weights were measured weekly and food intakes were measured at intervals. For *in vivo* evaluation of metabolic parameters, the mice were food-deprived for 4 h prior to experimental procedures except where noted. For tissue harvesting, mice were sacrificed, and tissues were immediately frozen in liquid nitrogen and stored at −80 °C until biochemical analysis, or were fixed for histology and immunohistochemistry. For the preparation of isolated adipocytes, freshly harvested adipose tissue was digested by collagenase in Krebs-Ringer bicarbonate (KRB) buffer (34). All animal studies were performed in accordance with the guidelines and under approval of the Institutional Review Committee for the Animal Care and Use of Boston University.

Cell Culture—MEF cells from *cavin-1*$^{-/-}$ and WT mice were isolated and cultured as previously described for obtaining Cav1-null MEFs (26). Cavin-1 overexpression in HEK293 cells was achieved as reported in Ref. 16.

Histology and Immunohistochemistry—Tissues were fixed with Z-Fix (Anatech Ltd.), embedded in paraffin, sectioned at a thickness of 6–8 μm, and stained with hematoxylin and eosin (H & E). For collagen detection, sections were stained with Masson's trichrome reagent as specified by the manufacturer (Sigma). Rat anti-mouse Mac-3 antibody (BD Biosciences) was used for Mac3 staining using standard procedures.

Tissue Lipid Content—Lipids were extracted by the Folch procedure (35), dried under N_2 and reconstituted in PBS (1% Triton). Total TG and cholesterol content was measured using commercial enzymatic assays (Pointe Scientific, Canton, MI).

Glucose and Fat Tolerance Tests—Mice were fasted overnight (16 h). For glucose tolerance tests, mice were injected intraperitoneally with glucose (1.5 g/kg body weight). Tail blood glucose was measured at various time points using a glucometer (Bayer). For the fat tolerance test, mice were given an oral bolus (20 μl/g body weight) of olive oil. Tail vein blood was sampled before and at various times after olive oil administration for determination of plasma TG levels by enzymatic assay.

Acute β-Adrenergic Stimulation in Vivo—Age-matched cavin-1-null mice and wild-type mice were fasted for 4 h and subjected to an intraperitoneal injection of isoproterenol (10 mg/kg) or saline. Blood was collected before and 20 min after injection for determination of free glycerol levels (Sigma) and free fatty acid levels (Biovision). The white adipose tissues were rapidly harvested and snap frozen in liquid N_2 for subsequent analysis.

Adipocyte Isolation and Lipolysis, Glucose Uptake, and FA Uptake—Primary adipocytes were isolated from epididymal fat pads by collagenase as described, in the presence of 200 nM adenosine (Sigma) (34). The isolated cells were filtered through a 250-μm nylon mesh and washed three times. Cell diameter was determined from photomicrographs, and the average fat cell weight was calculated (36). Total neutral lipid was measured as described (37). For lipolysis, aliquots (0.5 ml) of cell suspension (7%, *v*/*v*) were incubated with 4 μg/ml adenosine deaminase (Roche) and 20 nM (−)-N^6-(2-phenyl-isopropyl)-adenosine (Sigma) for basal lipolytic activity or 1 μM isoproterenol for stimulated activity. Glycerol released into the medium was determined as lipolytic activity using a fluorometric assay (38). Triplicate measurements were performed for each mouse and 6–7 mice of each genotype were tested. For glucose uptake, isolated adipocytes were washed in glucose-free KRH buffer with 4% BSA and 200 nM adenosine, then aliquots (0.4 ml) of cell suspension (10%, *v*/*v*) were incubated with or without insulin (1 nM) for 20 min before adding a glucose mixture (0.1 mM 2-deoxyglucose and 0.5 μCi/ml deoxy-D-glucose, 2-[1,2-^{3}H(*N*)]-) (PerkinElmer, NET 328) for 5 min. Uptake was terminated by transferring the cell suspension into a microfuge tube containing 100 μl of silicone oil and immediately spinning to separate cells from media. Radioactivity associated with the cells was measured with scintillation counting, and zero-time values were subtracted. The data were normalized to cell number and the rate of uptake was expressed as CPM per 10^6 cells per min. For fatty acid uptake, isolated adipocytes were suspended in KRH buffer (0.1% BSA) at a density of 30%. Transport of oleate was started by adding 90 μl of a mixed cell suspension to 10 μl of isotope solution (containing 0.5 μCi/ml ^{3}H-labeled oleate (PerkinElmer, NET 289) and oleate complexed to BSA at ratio of 2:1). Uptake was terminated at 15 s and 30 s, respectively by the addition of 5 ml of cold stop solution (200 μM Phloretin), and the cells were separated from medium by vacuum filtration using A/E glass filters. Cell-associated radioactivity was obtained by counting the washed filters (39, 40).

Cell incorporation of fatty acid was measured using ^{3}H-labeled oleate (Oleate: BSA 2:1) incubated with aliquots of 10% isolated adipocytes for 60 min. The cell suspension was transferred to a microfuge tube containing silicone oil and immediately spun to separate cells from media. Radioactivity associated with the cells was measured by scintillation counting.

LDH Release in Cultured Adipose Tissue—Epididymal fat pads of *cavin-1*$^{-/-}$ and WT mice were obtained by dissection,

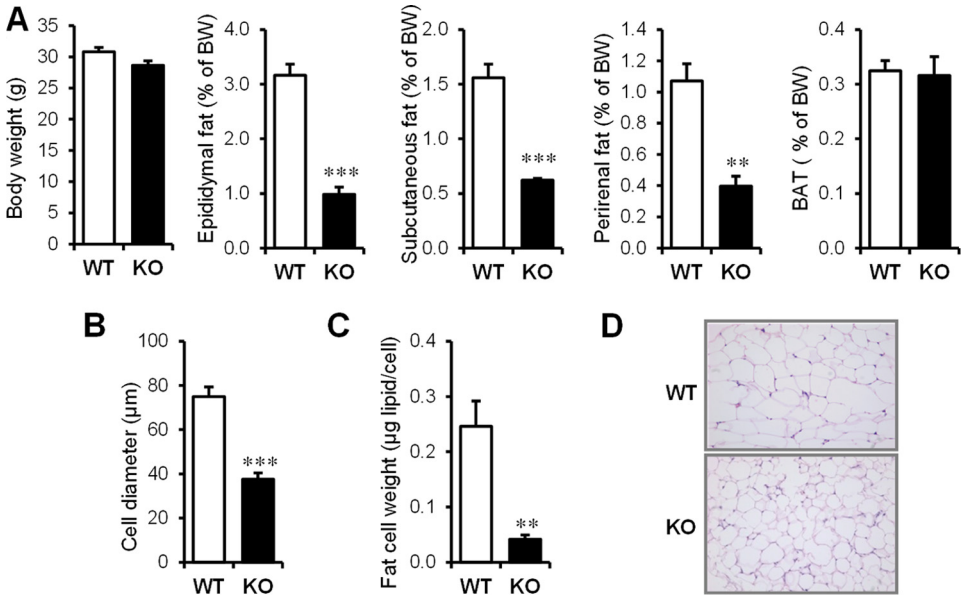

FIGURE 1. **Cavin-1 gene knock-out results in reduced fat pad weight and adipocyte size.** *A*, shown (*left* to *right*) is the total body weight and the percent body weight of epididymal, subcutaneous, and perirenal fat pads as well as BAT in 3-month-old male *Cavin-1*-null mice and their littermates (WT) ($n = 5–6$). *B*, average size of isolated adipocytes from 3-month-old *Cavin-1*-null mice and WT mice. The sizes of 200 randomly selected individual adipocytes from each mouse were determined from scaled images using SPOT software. A total of 1000 adipocytes from 5 mice per genotype were quantified and used for determining the average cell diameter size. *C*, fat content/cell from the same adipocytes of WT and *Cavin-1*-null mice is shown. Data are expressed as the mean ± S.E. ***, $p < 0.001$ for WT *versus* KO and **, $p < 0.01$. *D*, representative H&E staining of epididymal adipose tissue sections from *Cavin-1*-null (*KO*) and WT mice is shown at 20× magnification.

and ~50 mg of explants were incubated in KRB buffer at 37 °C for 2 h with gentle shaking. The medium was collected at the end of incubation, and LDH activity was measured using a commercial LDH cytotoxicity assay kit (Cayman Chemical Co., Ann Arbor, MI). Zero-time tissue pieces were homogenized in KRB containing 0.1% Triton to assess total intracellular LDH in the tissue.

Quantitative RT-PCR—Total RNA was isolated from indicated tissues or cells with TRIzol reagent (Invitrogen), and the cDNA was synthesized using Reverse Transcription System (Promega). Real-time PCR was performed with the ViiA7 detection system (Applied Biosystems) using Fast SYBR Green Master Mix (Applied Biosystems). Gene expression levels were normalized to 36B4 and presented relative to the wild type. The primer sequences are available upon request.

Immunoblot Analysis—Protein was extracted using RIPA lysis buffer, and the concentration was determined using a BCA protein assay kit (Pierce). The tissue homogenates were subjected to SDS-PAGE, and proteins were transferred to PVDF membranes. After blocking with 10% nonfat dry milk in PBST, the membranes were incubated with primary antibodies and then horseradish peroxidase-conjugated secondary antibodies (Sigma). Chemiluminescent signals were developed with enhanced reagents (PerkinElmer), followed by detection by Fujifilm LAS-4000 Image Analyzer. Primary antibodies used in these studies included rabbit polyclonal anti-cavin-1 (21st Century Biochemicals); monoclonal PTRF/cavin-1 (BD Transduction Laboratory); anti-c/EBPα, anti-SREBP-1c, anti-CGI-58 antibody (Proteintech Group. Inc), anti-phospho-HSL (Ser-563 and Ser-660) and anti-PKA substrates antibody (Cell Signaling Technology), anti-β-actin and tubulin antibodies (Sigma). Antibodies to UCP1, PGC-1α, COX-IV, and cyclophilin were kindly provided by Dr. Stephen Farmer (Boston University) and antibody to CD36 was kindly provided by Dr. Maria Fabbraio (Case Western University). Antibodies to perilipin-1 (rabbit polyclonal) (41), hormone-sensitive lipase (HSL) (42), and adipocyte triglyceride lipase (ATGL) (43) were described previously.

Statistics—Data are presented as means ± S.E. The significance of differences between groups was evaluated using ANOVA or 2-tailed unpaired Student's *t* test. A p value <0.05 was considered significant.

RESULTS

Cavin-1-null Mice Have Reduced Adipose Depot Mass and Smaller Fat Cells—We reported previously that 8–12-week-old male *cavin-1*$^{-/-}$ mice have a slight but nonsignificantly reduced body weight compared with their WT littermates (15), but they have significantly lower levels of overall adiposity. With a larger cohort of mice, we confirmed that *cavin-1*$^{-/-}$ and WT mice do not show significant differences in body weight (Fig. 1*A*) at this age, although we do find there is a tendency for *cavin-1*$^{-/-}$ mice to have lower body weights than WT littermates after 5 months of age (not shown). Epididymal, subcutaneous, and perirenal white fat depot weights were reduced by 60–70% in the null mice, but brown adipose tissue (BAT) mass was the same (Fig. 1*A*, *right most graph*). To determine the basis for the reduced adiposity, we measured cell diameters from each genotype for 200 randomly chosen perigonadal adipocytes. Adipocyte diameter follows a normal distribution in both knock-out and wild-type mice, but fat cells were significantly smaller in *cavin-1*$^{-/-}$ adipose tissue with the average cell diameters of *cavin-1*$^{-/-}$ fat cells being 37.6 ± 2.8 as compared with 75.0 ± 4.4 μm for WT adipocytes (Fig. 1*B*). The difference in fat content is even greater when expressed as fat cell weight

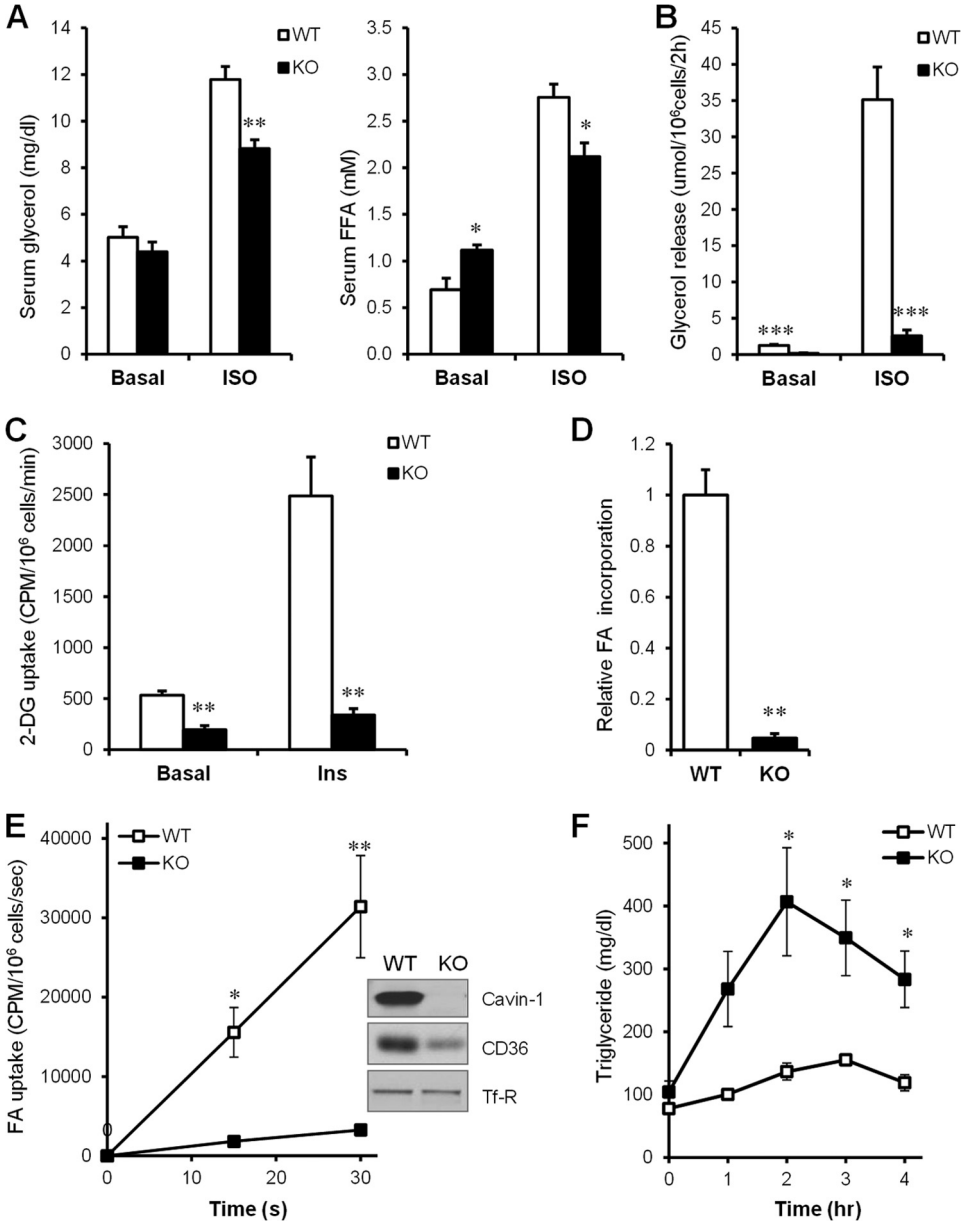

FIGURE 2. **Cavin-1 deficiency results in reduced isoproterenol-stimulated lipolysis, loss of insulin-stimulated glucose uptake, decreased fatty acid uptake and incorporation, and impaired fat tolerance.** *A*, serum free glycerol levels and free fatty acid levels in wild-type and knock-out mice before and 20 min after isoproterenol administration (10 mg/kg) ($n = 5–6$). *B*, basal and β-adrenergic receptor agonist-stimulated (isoproterenol, 1 μM) lipolysis, was measured as glycerol release over a 2-h period for isolated primary adipocytes from WT and *Cavin-1*-null mice. The lipolytic rate was normalized to adipocyte cell number ($n = 6–7$). *C*, primary adipocytes were treated with 1 nM insulin or not and 2-DOG uptake was determined as described under "Experimental Procedures" ($n = 4$). *D*, relative cell-associated radioactivity incorporation of oleate into lipid over a 60-min period in WT and *Cavin-1*-null adipocytes ($n = 3$). *E*, initial uptake kinetics of 33.3 μM [^{3}H]oleate into adipocytes, 15 s and 30 s from WT and *Cavin-1*-null mice ($n = 4$). *F*, oral fat tolerance test: mice were fasted for 16 h, followed by an oral bolus of olive oil (20 μl/g BW). Aliquots of tail vein blood were sampled at the times indicated after gavage for the determination of plasma TG levels ($n = 4–5$). Data are expressed as the mean ± S.E. *, $p < 0.05$; **, $p < 0.01$; ***, $p < 0.001$ for WT *versus* KO.

(Fig. 1*C*). H&E staining on fixed epididymal adipose tissue also confirmed the cell size difference *in situ*, as shown in Fig. 1*D*.

Cavin-1 Deficiency Results in Reduced Isoproterenol-stimulated Lipolysis, Loss of Insulin-stimulated Glucose Uptake and Reduced Fatty Acid Uptake and Incorporation into Lipid—To establish a metabolic explanation for the reduction of adipose tissue mass (15), we examined lipolysis *in vivo* (Fig. 2*A*) and in isolated adipocytes (Fig. 2*B*). Baseline serum glycerol levels were similar in the WT and *cavin-1*$^{-/-}$ mice while free FA levels were higher in *cavin-1*$^{-/-}$ mice as we previously reported, but there was a blunted response to isoproterenol administration in the knock-out (25% lower after 20 min), reflected by decreased levels of both free glycerol and free fatty acid. In isolated adipocytes *in vitro*, basal lipolysis per adipocyte was slightly lower in the knock-out than in WT, and the response to isoproterenol was markedly blunted so that rate of adrenergically stimulated lipolysis was ~85% lower in the knock-out cells. We previously showed *cavin-1*$^{-/-}$ mice have impaired insulin sensitivity, reduced GLUT4 expression, and lower levels of the insulin receptor signaling pathway components in adipose and muscle tissue (15). As shown in Fig. 2*C*, rates of basal 2-DOG uptake and the magnitude of the insulin-

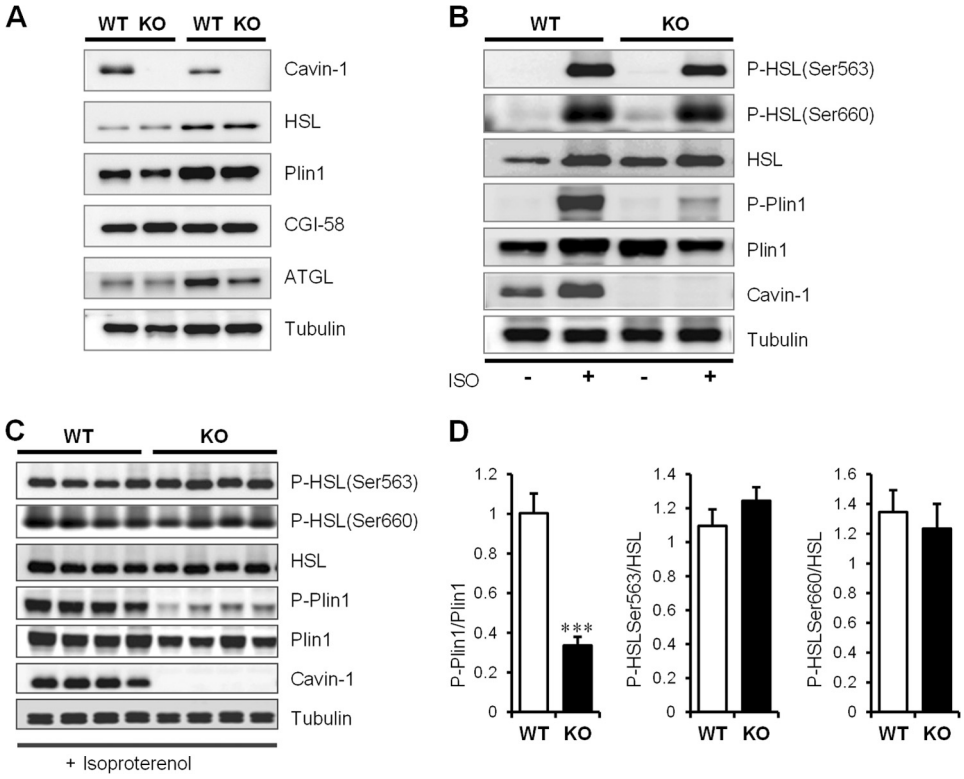

FIGURE 3. **Isoproterenol-stimulated perilipin-1 (Plin1) phosphorylation is blunted in fat cells lacking cavin-1.** *A*, Western blots showing the relative amounts of key lipolytic proteins from epididymal adipose tissue of 3-month-old male *Cavin-1*-null and WT mice. *B*, impaired Plin1 phosphorylation (P-Plin1) in response to isoproterenol stimulation *in vivo*. This is a representative Western blot showing total expression and phosphorylation levels of key lipolytic proteins from epididymal adipose tissue of *Cavin-1*-null and WT mice under basal or stimulated states. *C*, shown is a Western blot documenting the expression and phosphorylation levels of Plin-1 and HSL in isoproterenol stimulated epididymal adipose tissue from *Cavin-1*-null and WT mice and the indicated bands were quantitatively analyzed (*D*). Data were expressed as mean ± S.E. ***, $p < 0.001$ for WT *versus* KO.

stimulation uptake, which reflects transport, were markedly lower in the knock-out adipocytes. As glucose uptake and conversion to glyceride-glycerol is needed to esterify fatty acids, the *cavin-1*$^{-/-}$ fat cells would be expected to have lower triglyceride synthesis. We further examined the rates of free fatty acid uptake into adipocytes and incorporation into TG. We have previously reported decreased FA uptake in Cavin-1 knockdown 3T3-L1 adipocytes (16) and caveolin-1 has been suggested to function in FA uptake by localizing CD36 to caveolae where it can enhance FA uptake (44). Our results showed a markedly blunted initial rate of oleate uptake (Fig. 2*E*) and incorporation into cells (lipid) (Fig. 2*D*) in isolated *cavin-1*-null adipocytes and levels of CD36 protein were also substantially decreased. The impaired glucose and FA uptake explains the much lower triglyceride levels in *cavin-1*$^{-/-}$ fat cells, and hence we expected reduced clearance of an acute oral fat load. Consistent with this idea, the fat tolerance test showed a significantly greater increase in serum TG after a lipid gavage in the knock-out mice, suggesting decreased fat clearance (Fig. 2*F*).

Isoproterenol-stimulated Perilipin-1 (Plin1) Phosphorylation Is Blunted in Fat Cells Lacking Cavin-1—We next examined epididymal fat for selected proteins involved in the regulation of lipolysis (45) and found hormone sensitive lipase (HSL), Plin1, comparative gene identification-58 (CGI-58) and adipocyte triglyceride lipase (ATGL) levels were not significantly different between the *cavin-1*$^{-/-}$ and WT littermates (Fig. 3*A*). We then measured basal and β-adrenergic-activated phosphorylation events in adipose tissue and showed that phosphorylation of HSL was unaffected, but Plin1 phosphorylation was significantly reduced (Fig. 3*B*). Adrenergic stimulation was repeated for a cohort of 4 mice and HSL Ser-563 and Ser-660 sites were phosphorylated to the same extent in WT and *cavin-1*$^{-/-}$ mice, but Plin1 phosphorylation was reduced by ~70% in *cavin-1*-null adipose tissue (Fig. 3, *C* and *D*). This result suggests that absence of cavin-1 results in selective inhibition of Plin1 phosphorylation, but the upstream PKA signaling is not affected in these cells.

The Adipose Tissue of Cavin-1-null Mice Is Fibrotic, Macrophage-infiltrated, and Leaks LDH—Insulin resistance related to adipocytes may include contributions by macrophage-mediated inflammation, fibrosis caused by collagen deposition, and cell death/necrosis. Accordingly, we stained adipose tissue from WT and *cavin-1*$^{-/-}$ mice with trichrome for collagen (Fig. 4*A*), and Mac3 for macrophage infiltration (Fig. 4*B*) along with mRNA expression of macrophage markers F4/80 and CD68 (Fig. 4*C*). Lipotoxicity/cell leakiness was determined by measuring the release of LDH from adipose tissue explants (Fig. 4*D*) and isolated adipocytes (not shown). The data showed increased fibrosis, macrophage infiltration, and LDH release, respectively, for the *cavin-1*$^{-/-}$-derived adipose tissue as compared with the WT adipose tissues.

Cavin-1 has been reported to inhibit collagen gene expression by associating with a protein called binding factor of a type-1 collagen promoter (BFCOL1) (46). Accordingly we show in Fig. 4*E* that the expression of three collagen (*Col*) genes is

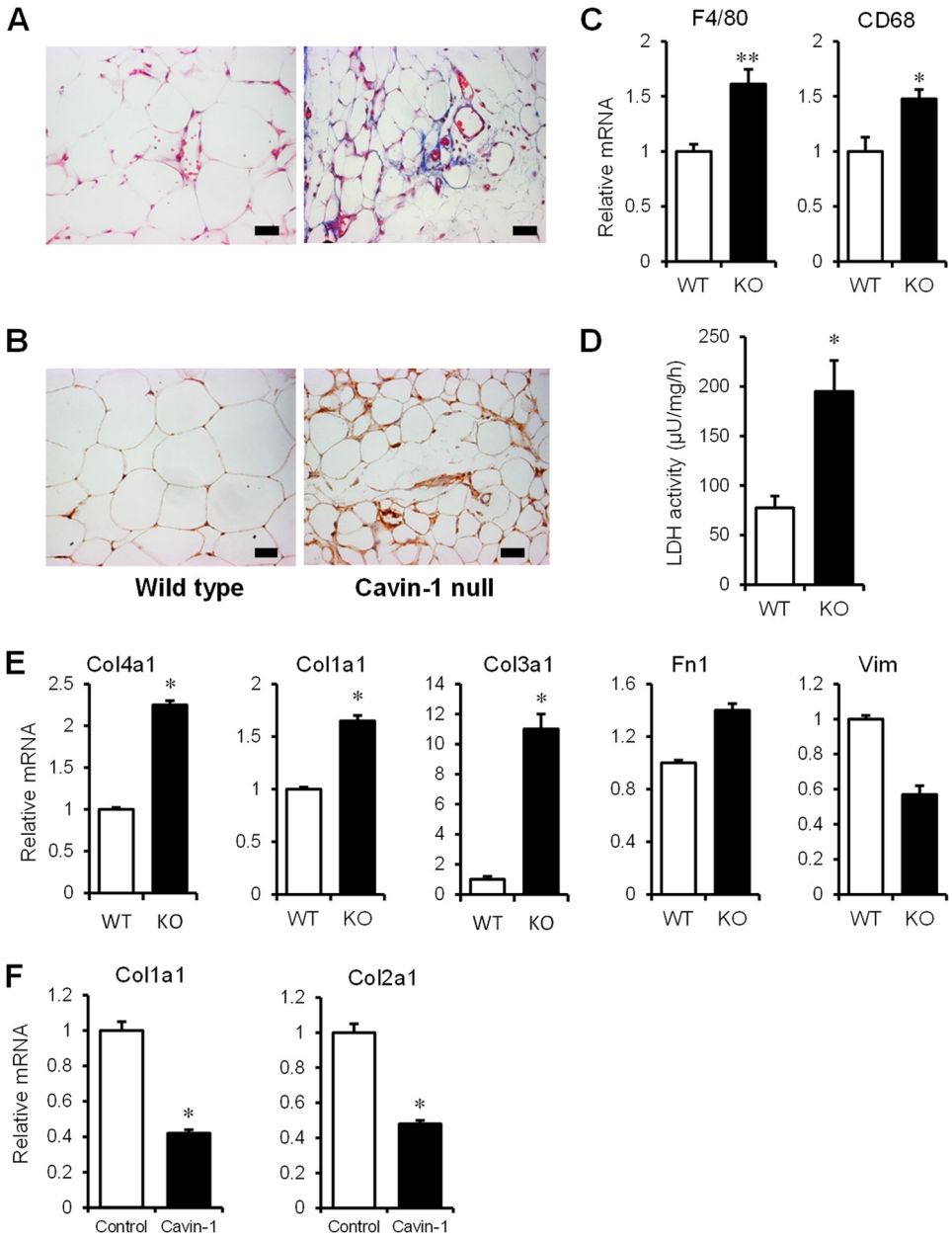

FIGURE 4. **The adipose tissue of *cavin-1*-null mice is fibrotic, macrophage infiltrated, and leaky.** *A*, adipose tissue sections for the 2 phenotypes were stained with Masson trichrome for collagen. *B*, macrophage marker Mac3 immunohistochemical staining of WT and KO adipose tissue. The pictures shown are representative of tissue from 3 or more mice. *C*, gene expression (mRNA) of macrophage markers F4/80 and CD68 in WT and KO adipose tissue ($n = 5$). *D*, LDH release from epididymal adipose tissue explants of WT and *Cavin-1* KO mice after 2 h incubation normalized to total LDH activity ($n = 4$). *E*, transcript levels of fibrosis markers were measured by qPCR. The genes are collagen 1a1 (Col1a1), Collagen 3a1 (Col3a1), collagen 4a1 (Col4a1), fibronectin (Fn1), and vimentin (Vim) in WT and Cavin-1-null MEFs. *F*, gene expression (mRNA) of col1a1 and collagen 2a1 (Col2a1) in Cavin-1-overexpressing HEK293 cells. *, $p < 0.05$; **, $p < 0.01$ for WT *versus* KO or Control *versus* Cavin-1-overexpressing cells.

up-regulated in *cavin-1*-null MEFs along with fibronectin1 (Fn1), whereas vimentin (Vim) is not. As might be expected, the opposite occurs in HEK293 cells overexpressing cavin-1 (Fig. 4*F*), namely two additional Col genes are down-regulated. These Col genes were all seen to be up-regulated in microarrays from cavin-1-null adipocytes (data not shown). Thus, the gene expression data of Fig. 4, *E* and *F* are consistent with the histological data of Fig. 4*A* and with a regulatory role for cavin-1/PTRF in collagen gene expression.

Cavin-1-null Mice Are Resistant to Diet-induced Obesity—To test whether *cavin-1*$^{-/-}$ mice could increase fat storage, mice were challenged with a high fat diet. As shown in Fig. 5*A*, WT mice gained more weight on the HF compared with the control chow diet, but the knock-out mice did not. The differences in body weight could not be explained by hypophagia, as daily average food intake (kcal/d) was similar in WT and knock-out mice on either diet (Fig. 5*C*). WT mice were considerably more glucose intolerant than the knock-out mice after high-fat feeding (Fig. 5*D*). The latter are mildly glucose intolerant whether or not they are on a HFD.

Livers from Cavin-1-null mice Are Steatotic, Which Is Not Worsened by HFD Whereas Skeletal Muscle from the Knockouts Fails to Accumulate Fat on Either Diet—We measured liver (Fig. 6*A*) and skeletal muscle lipid content (Fig. 6*B*) in WT and

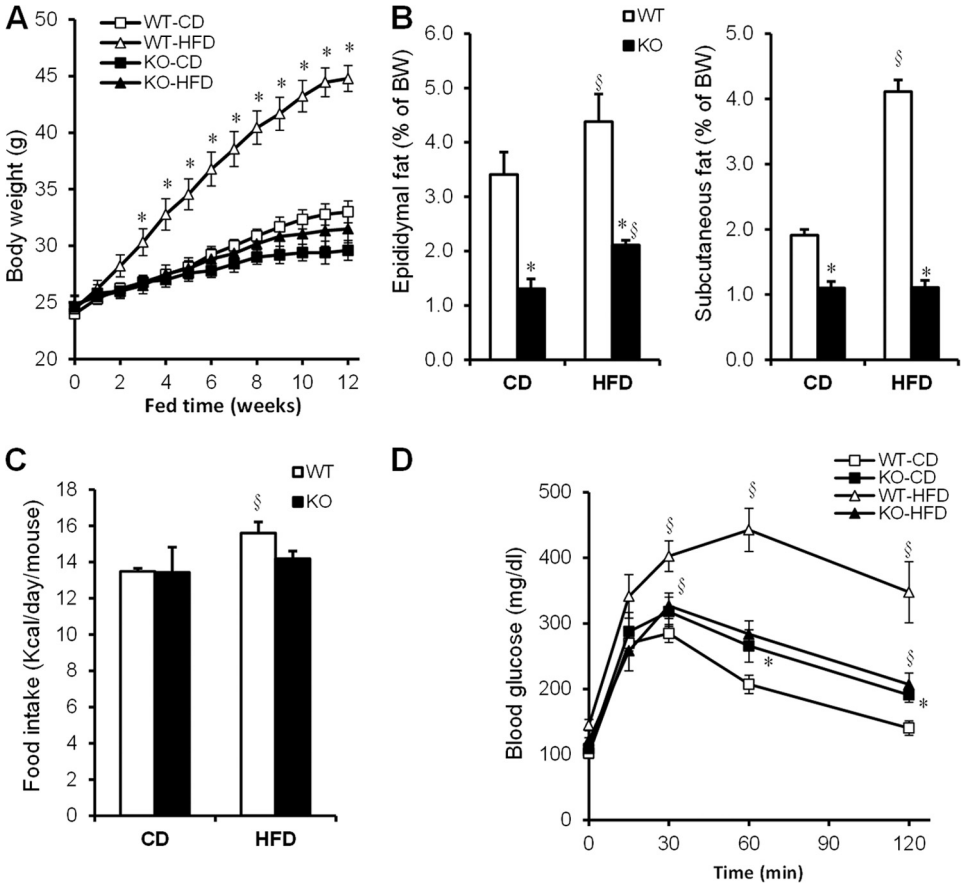

FIGURE 5. **Cavin-1 deficiency protects against HFD-induced obesity and glucose intolerance.** *A*, shown is the body weight as a function of time on a chow diet (*CD*) and HFD-fed wild-type and knock-out mice during a 12-week period. *Panel B* shows the percent of epididymal and subcutaneous fat pad weight of total body weight (*BW*) for the fat depots indicated. *C*, average food intake per mouse during a 2-week period is equal for the 2 genotypes. *D*, glucose tolerance (1.5 g/kg B.W.) was assessed in chow- and HF diet-fed WT and KO mice after an overnight fast ($n = 5$–9). Data were expressed as mean ± S.E. *, WT *versus* KO ($p < 0.05$); and §, CD *versus* HFD ($p < 0.05$).

cavin-1$^{-/-}$ mice and observed that the latter had slightly fattier livers than WT on chow, but liver fat content did not increase on a HFD while it significantly increased in WT on a HFD. Skeletal muscle from the knock-out animals did not accumulate fat under either diet, whereas the WT did when subjected to excess calories for 12 weeks. In confirmation of Fig. 6*A*, the expression level of the liver lipid droplet protein, Plin2 (45) is higher in the knock-out animals fed a chow diet but is essentially the same in both genotypes on a HFD (Fig. 6*C*). The mRNAs for selected genes involved in the regulation of hepatic lipogenesis (ACC, acetyl-CoA carboxylase; SREBP, sterol response element-binding protein) were also higher in livers of *cavin-1*$^{-/-}$ mice, but unlike WT mice, they were not increased following a HFD (Fig. 6*D*).

UCP1 Expression Is Induced in Mice Lacking Cavin-1 upon a HFD—The null mice do not gain any weight upon exposure to a HFD (Fig. 5*A*) despite normal food intake, which suggested that they may have enhanced fat oxidation under these circumstances. We determined that brown adipocytes, like white fat cells, were smaller in the null mice and remained smaller after a HFD as compared with WT (Fig. 7*A*). We then measured the expression of selected mitochondrial proteins in these animals (Fig. 7*B*) and observed that UCP1 levels were low in *cavin-1*$^{-/-}$ mice on a chow diet, but were markedly up-regulated after a HFD to the level of the WT mice. We also checked mRNA levels of BAT genes that regulate mitochondrial thermogenesis and biogenesis (Fig. 7, *C–E*) and found that peroxisome proliferator-activated receptor-α (PPARα), PPARγ coactivator-1A (PGC1-α), uncoupling protein (UCP1), and CCAAT/enhancer binding protein β (c/EBPβ) were all decreased in *cavin-1*$^{-/-}$ BAT, but were induced to the WT levels by a high fat challenge (Fig. 7*C*). A metabolic characteristics of brown adipocytes is their high rate of fatty acid oxidation that performs the beneficial function of expending excess energy, thus we examined the abundance of mRNAs for acyl-CoA dehydrogenases, which are important for fatty acid oxidation in mitochondria, including very long-chain acyl-CoA dehydrogenase (VLCAD), long-chain acyl-CoA dehydrogenase (LCAD), and medium-chain acyl-CoA dehydrogenase (MCAD). Those genes were all decreased in BAT of *cavin-1*$^{-/-}$ mice but were induced to the similar level as WT after high fat feeding.

DISCUSSION

Here we phenotypically characterize a novel model of lipodystrophy caused by cavin-1 deficiency, one that corresponds closely to the phenotype of humans lacking functional cavin-1 as described in patients from at least 4 distinct ethno-geographic regions of the globe (31–33, 47). The absence of cavin-1 protein in mice (15) and humans (31–33, 47) eliminates caveolae and causes a lipodystrophic phenotype entailing reduced

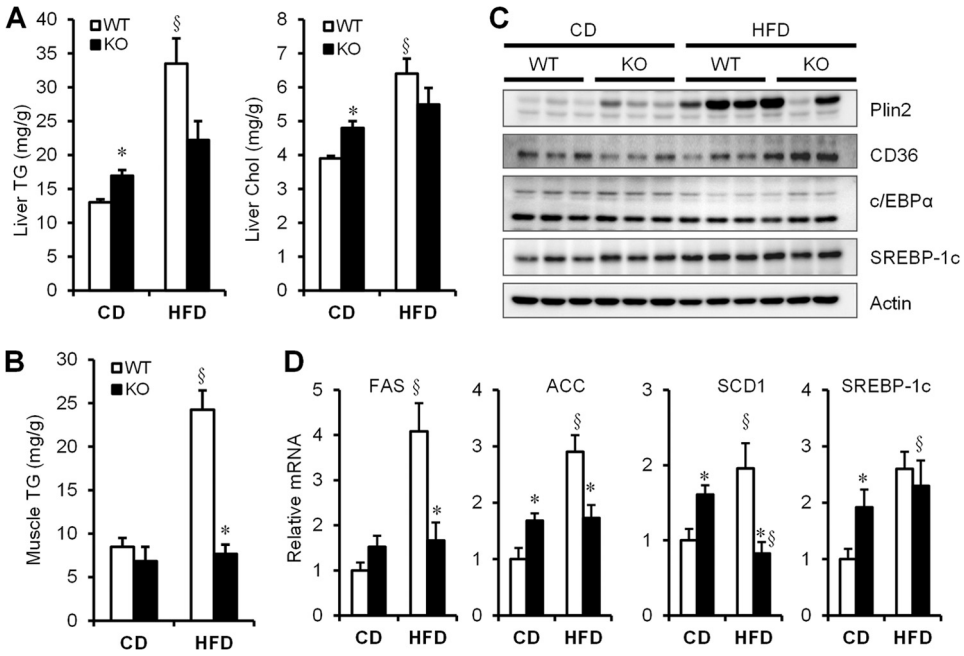

FIGURE 6. **Cavin-1-null mice are resistant to diet-induced hepatic steatosis and muscle fat accumulation.** *A*, hepatic concentrations of triglyceride and cholesterol in WT and KO mice fed with chow diet (*CD*) or a HFD for 12 weeks. *B*, triglyceride levels in muscle in WT and KO mice fed a CD or a HFD. *C*, representative Western blots ($n = 3$) of proteins isolated from liver of CD- and HFD- fed mice. *D*, relative expression of hepatic genes that regulate lipogenesis in liver, including FAS, ACC, SCD1, SREBP1-c ($n = 5–8$). Q-PCR data were normalized by the amount of 36B4 mRNA and expressed relative to the levels in WT-CD. * indicates significant differences ($p < 0.05$) between WT and KO; § indicates significant differences between CD and HFD.

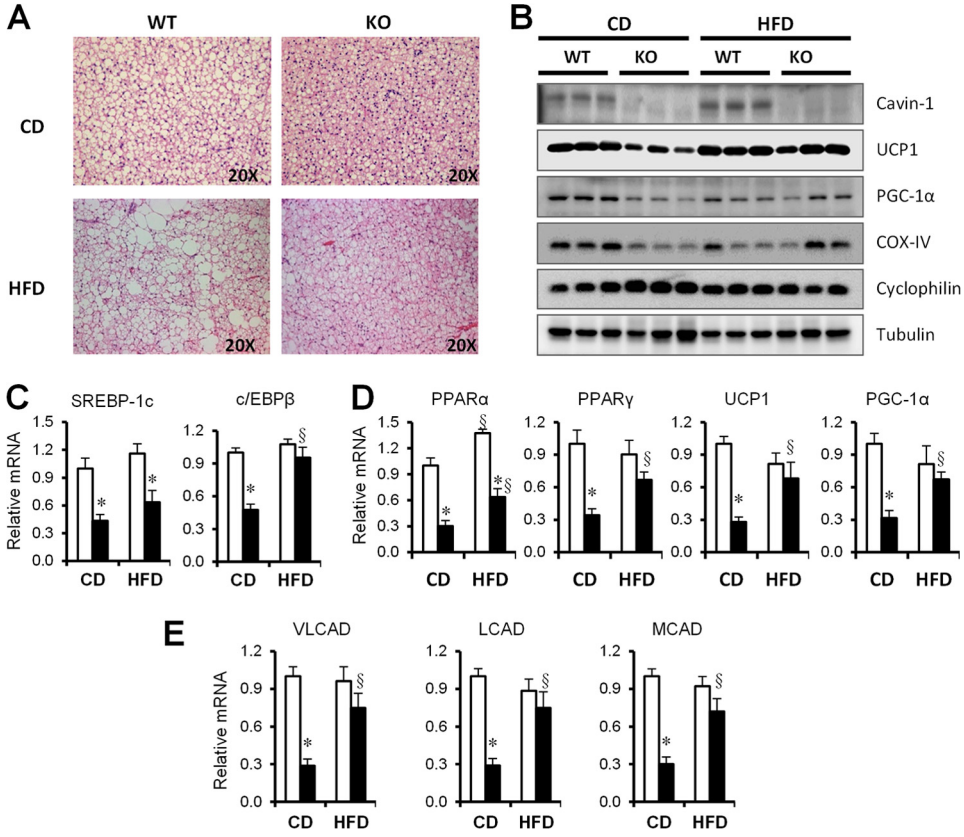

FIGURE 7. **The molecular characteristics of BAT differ in *cavin-1*-null and WT mice.** *A*, shown is a representative light microscopic images of H&E-stained sections of BAT following 12 weeks of a CD or a HFD. *B*, representative Western blots of the indicated proteins isolated from BAT of CD- and HFD-fed mice. *C*, quantitative real-time PCR analysis of the expression of genes associated with lipogenesis (SREBP-1c, c/EBPβ). *D*, mitochondrial biogenesis (PPARα, PPARγ, UCP1, PGC1-α) and *E*, fatty acid oxidation (VLCAD, LCAD, MCAD) in BAT of WT and *Cavin-1*-null mice fed a CD or a HFD ($n = 5–8$). Q-PCR data were normalized by the amount of 36B4 mRNA and expressed relative to the levels in WT. * indicates significant differences between WT and KO, and § indicates significant differences between CD and HFD ($p < 0.05$).

overall adiposity, impaired glucose tolerance, and hyperlipidemia. To better understand the phenotype, we described some of the underlying cellular/tissue defects that cause it, the predominant one being reduced adiposity in all major white fat depots due to small adipocytes and their inability to store lipid (Figs. 1–3) as well as other adipocyte pathologies (Fig. 4). Adipocytes lacking cavin-1 are markedly refractive to hormonal stimulation by insulin and isoproterenol, the latter due to diminished Plin1 phosphorylation despite normal adrenergic signaling toward HSL (Fig. 3). These cells also have a severely limited ability to utilize glucose (Fig. 2*C*), and because glycerol-3-P derived from glucose is needed to form the TG backbone, their capacity to esterify and store fatty acids is limited. We confirmed this *in vitro* in *cavin-1*-null adipocytes where fatty acid uptake (Fig. 2*E*) and incorporation (Fig. 2*D*) are greatly diminished and *in vivo* by a fat tolerance test (Fig. 2*F*). Thus the contribution of fat cells to the *cavin-1*-null phenotype is characterized by their remarkable incapacity to store lipid, and consequently, the observed hyperlipidemia. Considering our present and previous results, we postulate that adipocyte-related insulin resistance results from the imbalance of lipid uptake and lipolysis such that the former is even more impaired than the latter (8), and impaired lipid uptake is a major contributor to the lipodystrophic, insulin-resistant phenotype.

Both *cavin-1*-null and *Cav1*-null genotypes are dyslipidemic, but the onset of the phenotype is earlier and more pronounced in the former mice because, unlike the latter, they lack caveolae in all tissues including skeletal and cardiac muscle (8). In that regard, we showed that the machinery for insulin-stimulated glucose transport in muscle is down-regulated in *cavin-1*$^{-/-}$ mice (15). Although the liver lacks caveolae (17), liver function in *Cav1*-null animals appears to be phenotypically protective, and these mice show reduced levels of steatosis (48). On the other hand, *cavin-1*-null mice have mildly fatty livers on a normal diet (Fig. 6, *A* and *C*), and the level of liver fat is not exacerbated by high fat feeding. Muscle lipid content is unaffected by lack of caveolae (Fig. 5*B*) regardless of diet, which on the high fat diet, most likely reflects the reduced FA uptake and storage capacity of cells other than fat cells that lack caveolae (25), a property we have observed in cultured muscle cells where caveolins/caveolae have been knocked down.[5]

We subjected *cavin-1*$^{-/-}$ and WT mice to a HFD and observed that they had similar energy intake, but the former are resistant to weight gain and are equal in mass to WT on a chow diet at the same age of 20 weeks. As noted above, the null mice have slightly fattier livers at this time and slightly increased fat mass, but only in the epididymal fat depot (Fig. 5*B*). The nulls on a HFD also show no worsening of their mildly impaired glucose tolerance (Fig. 5*D*), a somewhat surprising result that suggests possible metabolic compensation in the *cavin-1*-null mice by a tissue other than white fat, muscle, or liver upon exposure to a caloric challenge. We therefore examined the properties of brown fat in WT and knock-out mice on chow and high fat diets. Brown adipose mass was unaffected by lack of cavin-1, but the brown fat cells, like white fat cells, were smaller and expressed lower levels of UCP1 (Fig. 7), a protein that has been suggested as a therapeutic target for the treatment of obesity by virtue of its ability to enhance FA oxidation (49). Interestingly, UCP1 levels are enhanced upon high fat feeding of the *cavin-1*$^{-/-}$ mice (Fig. 7), which likely contributes significantly to their resistance to a HFD-mediated weight gain.

Additional possible contributors to the pathophysiological phenotype of *cavin-1* knock-out mice are adipose tissue fibrosis and macrophage infiltration (50) as well as adipocyte fragility as indicated by higher LDH leakage (Fig. 4). The *in vitro* results for impaired lipolytic and insulin signaling are, however, necessarily independent of fibrosis and of the acute affects of macrophage infiltration. It is also possible that there are increased levels of autophagy in the *cavin-1* knock-out adipocytes as was reported for *Cav1*-null fat cells (51). Fibrosis and macrophage infiltration have been noted in Cav1-deficient adipocytes (52, 53) suggesting the lack of caveolae, *per se*, and not necessarily their individual protein components underlie adipocyte dysfunction in the mouse *in vivo*. This conclusion is also supported by developmental nutritional studies that reported similar changes in adipocytes for caveolae-related genes, Cav1, Cav2, cavin-1/PTRF, and cavin-3, as a function of diet (54). We cannot rule out, however, that the acute lack of hormonal responsiveness to lipolytic stimulation *in vitro* (Fig. 2) may have different contributions from the individual caveolae proteins. Indeed, we show here that transfected cavin-1 has effects in HEK293 cells (Fig. 4*F*), and these cells do not express the other caveolae proteins (16).

An impairment of the lipolytic response to isoproterenol was more marked in isolated cell incubations than in the *in vivo* test. Steady state plasma glycerol and FFA levels at a single time point after isoproterenol treatment may not accurately reflect the rate of appearance of glycerol and studies using tracer methods to assess more accurately assess turnover rates are needed. Also, basal lipolysis in the *in vitro* study was assessed under conditions of high adenosine that clamp cAMP at a very low levels; the situation *in vivo* likely differs.

Mechanistic information concerning how caveolae components participate in the regulation of lipolysis is relatively scarce and contradictory in part. Cohen *et al.* proposed that a ternary complex of Cav1-perilipin-PKA was required for hormonal-stimulated lipolysis, which would therefore be absent in *Cav1*-null adipocytes and would result in reduced Plin-1 phosphorylation and decreased stimulated lipolysis (55). However, in *Cav1*-null cultured adipocytes derived from *Cav1*-null MEFs, ISO-stimulated PKA-dependent phosphorylation of Plin-1 is normal and subsequent lipolytic stimulation in these cells is actually slightly but significantly greater than in these cells "rescued" by the re-introduction (by transfection) of Cav1 (26). Hence it seems unlikely that a Cav1-perilipin-PKA complex is required for regulated adipocyte lipolysis. Cavin-1 is possibly a better candidate for directly participating in lipolysis as it has been shown to be phosphorylated upon adrenergic stimulation (56), albeit at significantly later times than HSL and perilipin when lipolysis is well underway,[6] and experiments are under-

[5] S. Ding *et al.*, unpublished data.

[6] L. Liu and P. F. Pilch, unpublished data.

way to characterize possible molecular interactions responsible for the cavin-1 dependence of hormonal-regulated lipolysis.

We do however provide some new insight into the mechanism of fibrosis in the *cavin-1*-null mice, namely that cavin-1 regulates collagen gene expression (Fig. 4, *E* and *F*). Indeed, we saw a significant enhancement of collagen gene expression in microarrays of adipose tissue (data not shown) that we verified here by qPCR. Whether or not this is due to direct interaction of cavin-1 with BFCOL1 on the collagen promoter (46) remains to be determined as attempts to coimmunoprecipitate these proteins have as yet been unsuccessful. Moreover, it is likely that the effects of cavin-1/PTRF are also manifest in its regulation of ribosomal RNA (57, 58), and this possibility is also under experimental scrutiny.

Genetic lipodystrophies (59) like those due to lack of cavin-1 are relatively rare in the human population but the heterozygous condition will be much more prevalent, and there are data suggesting that caveolin-1 expression is down-regulated in adipocytes from obese humans (60). Thus it will be of interest to study the expression of the caveolae protein components including cavin-1 and cavin-2 in mouse models of diet-induced obesity and in *cavin-1*$^{+/-}$ mice, since the *cavin-1*-null animals resemble humans closely in their metabolic properties. Such studies are underway and preliminary data indicates that mice heterozygous for cavin-1 have glucose intolerance more severe than their WT counterparts.

REFERENCES

1. Napolitano, L. (1963) The Differentiation of White Adipose Cells. An Electron Microscope Study. *J. Cell Biol.* **18,** 663–679
2. Cushman, S. W. (1970) Structure-function relationships in the adipose cell. I. Ultrastructure of the isolated adipose cell. *J. Cell Biol.* **46,** 326–341
3. Carpentier, J. L., Perrelet, A., and Orci, L. (1976) Effects of insulin, glucagon, and epinephrine on the plasma membrane of the white adipose cell: a freeze-fracture study. *J. Lipid Res.* **17,** 335–342
4. Scherer, P. E., Lisanti, M. P., Baldini, G., Sargiacomo, M., Mastick, C. C., and Lodish, H. F. (1994) Induction of caveolin during adipogenesis and association of GLUT4 with caveolin-rich vesicles. *J. Cell Biol.* **127,** 1233–1243
5. Kandror, K. V., Stephens, J. M., and Pilch, P. F. (1995) Expression and compartmentalization of caveolin in adipose cells: coordinate regulation with and structural segregation from GLUT4. *J. Cell Biol.* **129,** 999–1006
6. Rothberg, K. G., Heuser, J. E., Donzell, W. C., Ying, Y. S., Glenney, J. R., and Anderson, R. G. (1992) Caveolin, a protein component of caveolae membrane coats. *Cell* **68,** 673–682
7. Pilch, P. F., Souto, R. P., Liu, L., Jedrychowski, M. P., Berg, E. A., Costello, C. E., and Gygi, S. P. (2007) Cellular spelunking: exploring adipocyte caveolae. *J. Lipid Res.* **48,** 2103–2111
8. Pilch, P. F., and Liu, L. (2011) Fat caves: caveolae, lipid trafficking and lipid metabolism in adipocytes. *Trends Endocrinol. Metab.* **22,** 318–324
9. Hansen, C. G., and Nichols, B. J. (2010) Exploring the caves: cavins, caveolins and caveolae. *Trends Cell Biol.* **20,** 177–186
10. Hansen, C. G., Bright, N. A., Howard, G., and Nichols, B. J. (2009) SDPR induces membrane curvature and functions in the formation of caveolae. *Nat. Cell Biol.* **11,** 807–814
11. Bastiani, M., and Parton, R. G. (2010) Caveolae at a glance. *J. Cell Sci.* **123,** 3831–3836
12. Thorn, H., Stenkula, K. G., Karlsson, M., Ortegren, U., Nystrom, F. H., Gustavsson, J., and Stralfors, P. (2003) Cell surface orifices of caveolae and localization of caveolin to the necks of caveolae in adipocytes. *Mol. Biol. Cell* **14,** 3967–3976
13. Breen, M. R., Camps, M., Carvalho-Simoes, F., Zorzano, A., and Pilch, P. F. (2012) Cholesterol depletion in adipocytes causes caveolae collapse concomitant with proteosomal degradation of cavin-2 in a switch-like fashion. *PloS one* **7,** e34516
14. Hill, M. M., Bastiani, M., Luetterforst, R., Kirkham, M., Kirkham, A., Nixon, S. J., Walser, P., Abankwa, D., Oorschot, V. M., Martin, S., Hancock, J. F., and Parton, R. G. (2008) PTRF-Cavin, a conserved cytoplasmic protein required for caveola formation and function. *Cell* **132,** 113–124
15. Liu, L., Brown, D., McKee, M., Lebrasseur, N. K., Yang, D., Albrecht, K. H., Ravid, K., and Pilch, P. F. (2008) Deletion of Cavin/PTRF causes global loss of caveolae, dyslipidemia, and glucose intolerance. *Cell Metab.* **8,** 310–317
16. Liu, L., and Pilch, P. F. (2008) A critical role of cavin (polymerase I and transcript release factor) in caveolae formation and organization. *J. Biol. Chem.* **283,** 4314–4322
17. Bastiani, M., Liu, L., Hill, M. M., Jedrychowski, M. P., Nixon, S. J., Lo, H. P., Abankwa, D., Luetterforst, R., Fernandez-Rojo, M., Breen, M. R., Gygi, S. P., Vinten, J., Walser, P. J., North, K. N., Hancock, J. F., Pilch, P. F., and Parton, R. G. (2009) MURC/Cavin-4 and cavin family members form tissue-specific caveolar complexes. *J. Cell Biol.* **185,** 1259–1273
18. McMahon, K. A., Zajicek, H., Li, W. P., Peyton, M. J., Minna, J. D., Hernandez, V. J., Luby-Phelps, K., and Anderson, R. G. (2009) SRBC/cavin-3 is a caveolin adapter protein that regulates caveolae function. *EMBO J.* **28,** 1001–1015
19. Razani, B., Wang, X. B., Engelman, J. A., Battista, M., Lagaud, G., Zhang, X. L., Kneitz, B., Hou, H., Jr., Christ, G. J., Edelmann, W., and Lisanti, M. P. (2002) Caveolin-2-deficient mice show evidence of severe pulmonary dysfunction without disruption of caveolae. *Mol. Cell Biol.* **22,** 2329–2344
20. Hansen, C. G., Shvets, E., Howard, G., Riento, K., and Nichols, B. J. (2013) Deletion of cavin genes reveals tissue-specific mechanisms for morphogenesis of endothelial caveolae. *Nat. Commun* **4,** 1831
21. Ikonen, E., Heino, S., and Lusa, S. (2004) Caveolins and membrane cholesterol. *Biochem. Soc. Trans.* **32,** 121–123
22. Ost, A., Ortegren, U., Gustavsson, J., Nystrom, F. H., and Strålfors, P. (2005) Triacylglycerol is synthesized in a specific subclass of caveolae in primary adipocytes. *J. Biol. Chem.* **280,** 5–8
23. Brown, D. A. (2006) Lipid rafts, detergent-resistant membranes, and raft targeting signals. *Physiology* **21,** 430–439
24. Meshulam, T., Simard, J. R., Wharton, J., Hamilton, J. A., and Pilch, P. F. (2006) Role of caveolin-1 and cholesterol in transmembrane fatty acid movement. *Biochemistry* **45,** 2882–2893
25. Simard, J. R., Meshulam, T., Pillai, B. K., Kirber, M. T., Brunaldi, K., Xu, S., Pilch, P. F., and Hamilton, J. A. (2010) Caveolins sequester FA on the cytoplasmic leaflet of the plasma membrane, augment triglyceride formation, and protect cells from lipotoxicity. *J. Lipid Res.* **51,** 914–922
26. Meshulam, T., Breen, M. R., Liu, L., Parton, R. G., and Pilch, P. F. (2011) Caveolins/caveolae protect adipocytes from fatty acid-mediated lipotoxicity. *J. Lipid Res.* **52,** 1526–1532
27. Cohen, A. W., Razani, B., Wang, X. B., Combs, T. P., Williams, T. M., Scherer, P. E., and Lisanti, M. P. (2003) Caveolin-1-deficient mice show insulin resistance and defective insulin receptor protein expression in adipose tissue. *Am. J. Physiol. Cell Physiol.* **285,** C222–C235
28. Razani, B., Combs, T. P., Wang, X. B., Frank, P. G., Park, D. S., Russell, R. G., Li, M., Tang, B., Jelicks, L. A., Scherer, P. E., and Lisanti, M. P. (2002) Caveolin-1-deficient mice are lean, resistant to diet-induced obesity, and show hypertriglyceridemia with adipocyte abnormalities. *J. Biol. Chem.* **277,** 8635–8647
29. Cao, H., Alston, L., Ruschman, J., and Hegele, R. A. (2008) Heterozygous CAV1 frameshift mutations (MIM 601047) in patients with atypical partial lipodystrophy and hypertriglyceridemia. *Lipids Health Dis.* **7,** 3
30. Kim, C. A., Delépine, M., Boutet, E., El Mourabit, H., Le Lay, S., Meier, M., Nemani, M., Bridel, E., Leite, C. C., Bertola, D. R., Semple, R. K., O'Rahilly, S., Dugail, I., Capeau, J., Lathrop, M., and Magré, J. (2008) Association of a homozygous nonsense caveolin-1 mutation with Berardinelli-Seip congenital lipodystrophy. *J. Clin. Endocrinol. Metab.* **93,** 1129–1134
31. Hayashi, Y. K., Matsuda, C., Ogawa, M., Goto, K., Tominaga, K., Mitsuhashi, S., Park, Y. E., Nonaka, I., Hino-Fukuyo, N., Haginoya, K., Sugano, H., and Nishino, I. (2009) Human PTRF mutations cause secondary deficiency of caveolins resulting in muscular dystrophy with generalized lipodystrophy. *J. Clin. Invest.* **119,** 2623–2633
32. Rajab, A., Straub, V., McCann, L. J., Seelow, D., Varon, R., Barresi, R.,

Schulze, A., Lucke, B., Lützkendorf, S., Karbasiyan, M., Bachmann, S., Spuler, S., and Schuelke, M. (2010) Fatal cardiac arrhythmia and long-QT syndrome in a new form of congenital generalized lipodystrophy with muscle rippling (CGL4) due to PTRF-CAVIN mutations. *PLoS Genet* **6,** e1000874

33. Shastry, S., Delgado, M. R., Dirik, E., Turkmen, M., Agarwal, A. K., and Garg, A. (2010) Congenital generalized lipodystrophy, type 4 (CGL4) associated with myopathy due to novel PTRF mutations. *Am. J. Med. Genet. A* **152A,** 2245–2253
34. Shaughnessy, S., Smith, E. R., Kodukula, S., Storch, J., and Fried, S. K. (2000) Adipocyte metabolism in adipocyte fatty acid binding protein knock-out mice (aP2−/−) after short-term high-fat feeding: functional compensation by the keratinocyte [correction of keritinocyte] fatty acid binding protein. *Diabetes* **49,** 904–911
35. Folch, J., Lees, M., and Sloane Stanley, G. H. (1957) A simple method for the isolation and purification of total lipides from animal tissues. *J. Biol. Chem.* **226,** 497–509
36. Goldrick, R. B. (1967) Morphological changes in the adipocyte during fat deposition and mobilization. *Am. J. Physiol.* **212,** 777–782
37. Dole, V. P., and Meinertz, H. (1960) Microdetermination of long-chain fatty acids in plasma and tissues. *J. Biol. Chem.* **235,** 2595–2599
38. Laurell, S., and Tibbling, G. (1966) An enzymatic fluorometric micromethod for the determination of glycerol. *Clin. Chim. Acta* **13,** 317–322
39. Febbraio, M., Abumrad, N. A., Hajjar, D. P., Sharma, K., Cheng, W., Pearce, S. F., and Silverstein, R. L. (1999) A null mutation in murine CD36 reveals an important role in fatty acid and lipoprotein metabolism. *J. Biol. Chem.* **274,** 19055–19062
40. Abumrad, N. A., Perkins, R. C., Park, J. H., and Park, C. R. (1981) Mechanism of long chain fatty acid permeation in the isolated adipocyte. *J. Biol. Chem.* **256,** 9183–9191
41. Gross, D. N., Miyoshi, H., Hosaka, T., Zhang, H. H., Pino, E. C., Souza, S., Obin, M., Greenberg, A. S., and Pilch, P. F. (2006) Dynamics of lipid droplet-associated proteins during hormonally stimulated lipolysis in engineered adipocytes: stabilization and lipid droplet binding of adipocyte differentiation-related protein/adipophilin. *Mol. Endocrinol.* **20,** 459–466
42. Souza, S. C., Muliro, K. V., Liscum, L., Lien, P., Yamamoto, M. T., Schaffer, J. E., Dallal, G. E., Wang, X., Kraemer, F. B., Obin, M., and Greenberg, A. S. (2002) Modulation of hormone-sensitive lipase and protein kinase A-mediated lipolysis by perilipin A in an adenoviral reconstituted system. *J. Biol. Chem.* **277,** 8267–8272
43. Miyoshi, H., Perfield, J. W., 2nd, Souza, S. C., Shen, W. J., Zhang, H. H., Stancheva, Z. S., Kraemer, F. B., Obin, M. S., and Greenberg, A. S. (2007) Control of adipose triglyceride lipase action by serine 517 of perilipin A globally regulates protein kinase A-stimulated lipolysis in adipocytes. *J. Biol. Chem.* **282,** 996–1002
44. Ring, A., Le Lay, S., Pohl, J., Verkade, P., and Stremmel, W. (2006) Caveolin-1 is required for fatty acid translocase (FAT/CD36) localization and function at the plasma membrane of mouse embryonic fibroblasts. *Biochim. Biophys. Acta* **1761,** 416–423
45. Greenberg, A. S., Coleman, R. A., Kraemer, F. B., McManaman, J. L., Obin, M. S., Puri, V., Yan, Q. W., Miyoshi, H., and Mashek, D. G. (2011) The role of lipid droplets in metabolic disease in rodents and humans. *J. Clin. Investig.* **121,** 2102–2110
46. Hasegawa, T., Takeuchi, A., Miyaishi, O., Xiao, H., Mao, J., and Isobe, K. (2000) PTRF (polymerase I and transcript-release factor) is tissue-specific and interacts with the BFCOL1 (binding factor of a type-I collagen promoter) zinc-finger transcription factor which binds to the two mouse type-I collagen gene promoters. *Biochem. J.* **347,** 55–59
47. Dwianingsih, E. K., Takeshima, Y., Itoh, K., Yamauchi, Y., Awano, H., Malueka, R. G., Nishida, A., Ota, M., Yagi, M., and Matsuo, M. (2010) A Japanese child with asymptomatic elevation of serum creatine kinase shows PTRF-CAVIN mutation matching with congenital generalized lipodystrophy type 4. *Mol. Genet Metab.* **101,** 233–237
48. Asterholm, I. W., Mundy, D. I., Weng, J., Anderson, R. G., and Scherer, P. E. (2012) Altered mitochondrial function and metabolic inflexibility associated with loss of caveolin-1. *Cell Metab.* **15,** 171–185
49. Nedergaard, J., and Cannon, B. (2010) The changed metabolic world with human brown adipose tissue: therapeutic visions. *Cell Metab.* **11,** 268–272
50. Govender, P., Romero, F., Shah, D., Paez, J., Ding, S. Y., Liu, L., Gower, A., Baez, E., Aly, S. S., Pilch, P., and Summer, R. (2013) Cavin-1; a regulator of lung function and macrophage phenotype. *PloS one* **8,** e62045
51. Le Lay, S., Briand, N., Blouin, C. M., Chateau, D., Prado, C., Lasnier, F., Le Liepvre, X., Hajduch, E., and Dugail, I. (2010) The lipoatrophic caveolin-1 deficient mouse model reveals autophagy in mature adipocytes. *Autophagy* **6,** 754–763
52. Briand, N., Le Lay, S., Sessa, W. C., Ferré, P., and Dugail, I. (2011) Distinct roles of endothelial and adipocyte caveolin-1 in macrophage infiltration and adipose tissue metabolic activity. *Diabetes* **60,** 448–453
53. Martin, S., Fernandez-Rojo, M. A., Stanley, A. C., Bastiani, M., Okano, S., Nixon, S. J., Thomas, G., Stow, J. L., and Parton, R. G. (2012) Caveolin-1 deficiency leads to increased susceptibility to cell death and fibrosis in white adipose tissue: characterization of a lipodystrophic model. *PloS one* **7,** e46242
54. Kozak, L. P., Newman, S., Chao, P. M., Mendoza, T., and Koza, R. A. (2010) The early nutritional environment of mice determines the capacity for adipose tissue expansion by modulating genes of caveolae structure. *PLoS One* **5,** e11015
55. Cohen, A. W., Razani, B., Schubert, W., Williams, T. M., Wang, X. B., Iyengar, P., Brasaemle, D. L., Scherer, P. E., and Lisanti, M. P. (2004) Role of caveolin-1 in the modulation of lipolysis and lipid droplet formation. *Diabetes* **53,** 1261–1270
56. Aboulaich, N., Chui, P. C., Asara, J. M., Flier, J. S., and Maratos-Flier, E. (2011) Polymerase I and Transcript Release Factor Regulates Lipolysis Via a Phosphorylation-Dependent Mechanism. *Diabetes*. **60,** 757–765
57. Jansa, P., Burek, C., Sander, E. E., and Grummt, I. (2001) The transcript release factor PTRF augments ribosomal gene transcription by facilitating reinitiation of RNA polymerase I. *Nucleic Acids Res.* **29,** 423–429
58. Jansa, P., Mason, S. W., Hoffmann-Rohrer, U., and Grummt, I. (1998) Cloning and functional characterization of PTRF, a novel protein which induces dissociation of paused ternary transcription complexes. *EMBO J.* **17,** 2855–2864
59. Garg, A. (2011) Clinical review#: Lipodystrophies: genetic and acquired body fat disorders. *J. Clin. Endocrinol. Metab.* **96,** 3313–3325
60. Fernandez-Real, J. M., Catalan, V., Moreno-Navarrete, J. M., Gomez-Ambrosi, J., Ortega, F. J., Rodriguez-Hermosa, J. I., Ricart, W., and Fruhbeck, G. (2010) Study of caveolin-1 gene expression in whole adipose tissue and its subfractions and during differentiation of human adipocytes. *Nutr. Metab.* **7,** 20